nature climate change

LETTERS

PUBLISHED ONLINE: 3 AUGUST 2015 | DOI: 10.1038/NCLIMATE2747

An end-to-end assessment of extreme weather impacts on food security

Erik Chavez[1,2*], Gordon Conway[1], Michael Ghil[3,4] and Marc Sadler[5]

Both governments and the private sector urgently require better estimates of the likely incidence of extreme weather events[1], their impacts on food crop production and the potential consequent social and economic losses[2]. Current assessments of climate change impacts on agriculture mostly focus on average crop yield vulnerability[3] to climate and adaptation scenarios[4,5]. Also, although new-generation climate models have improved and there has been an exponential increase in available data[6], the uncertainties in their projections over years and decades, and at regional and local scale, have not decreased[7,8]. We need to understand and quantify the non-stationary, annual and decadal climate impacts using simple and communicable risk metrics[9] that will help public and private stakeholders manage the hazards to food security. Here we present an 'end-to-end' methodological construct based on weather indices and machine learning that integrates current understanding of the various interacting systems of climate, crops and the economy to determine short- to long-term risk estimates of crop production loss, in different climate and adaptation scenarios. For provinces north and south of the Yangtze River in China, we have found that risk profiles for crop yields that translate climate into economic variability follow marked regional patterns, shaped by drivers of continental-scale climate. We conclude that to be cost-effective, region-specific policies have to be tailored to optimally combine different categories of risk management instruments.

An increasing body of scientific evidence, derived from both observations and model simulations, indicates that the climate system never was, nor is it likely to ever be, statistically stationary[10]. Moreover, statistical characterization of slowly changing weather extremes is fraught with difficulties[11]. These stem partly from the potentially large effects caused by lack of stationarity and partly from the existence of complex nonlinear processes and threshold effects. The assessment and the prediction of such effects, both deterministic and stochastic, on weather extremes depend on a number of interconnected drivers. For example, changes in weather variability season-to-season and year-to-year that affects food production derive from shifts in the statistics of decade-to-decade climate processes[12,13]. Thus, changes in the large-scale climate processes that drive both regional and global climate variability affect the annual onset of rainfall in the tropics and subtropics, as well as rainfall patterns in temperate latitudes, thus playing a significant role in the variability of regional rain-fed crop production[14]. The risk estimation methodology proposed here integrates large- and small-scale information, and is based on both observed and simulated data for weather, climate, crop vulnerability and economic conditions.

The overall, end-to-end methodological construct is illustrated in Fig. 1. It relies on machine learning involving weather indices that characterize the vulnerability of crops to weather variability in different technological scenarios (Fig. 1a).

We here used a stochastic 'weather-within-climate' downscaling approach that quantifies the interaction of low- and high-frequency climate variability (Fig. 1b) to determine the crop loss risk profiles (Fig. 1d) for future climate scenarios. These are then used to model the direct and indirect economic impacts subject to supply loss shock (Fig. 1e) and to determine optimum mix of risk transfer and mitigation policies in a particular region or country (Fig. 1f). We assessed the potential of this methodological construct by using data for weather, crops and the economy in four provinces (Shandong, Hebei, Guangdong and Guangxi) of the People's Republic of China, north and south of the Yangtze River.

Existing integrated assessment models (IAMs) have attempted to provide first estimates of future possible costs of climate impacts on the economy subject to different global warming scenarios[15,16]. However, the sensitivity of these IAMs to individual economic parameters, such as the discount rate, has limited their usefulness. Taking this into account, the methodology presented in Fig. 1 focuses on the economic impacts driven by the local and regional characteristics of weather variability and climate state changes, the local response of the system considered (for example, the crop production sector), and different scenarios of technological risk mitigation.

Weather indices were devised as proxies of physical crop response to two of the main drivers of yield variability, namely precipitation variability and exposure to excess temperatures. Other hazards, such as cold shocks or radiation variability, are not considered here for lack of space. Observed historical daily weather data and soil databases for the studied provinces are used to simulate crop yields using mechanistic crop modelling. Daily precipitation and temperature data are used to build pixel-level databases of precipitation and temperature variability indices. Each index captures exposure to deficit precipitation or excess temperature during different time intervals of crop growth.

The translation of the metrics of physical-loss risk into metrics of direct and indirect economic loss is carried out through macroeconomic modelling of exogenous, supply-side shocks. Probabilistic and scenario-based risk modelling is cascaded from climate to agricultural, and finally economic loss through data clustering, by using machine learning techniques of recursive partitioning[17] and nonhomogeneous hidden Markov models[18] (NHMMs), as illustrated in Supplementary Fig. 1. The joint effects of precipitation variability and excess temperature were modelled through stochastic-copula dependency; see Methods and

[1]Imperial College London, Centre for Environmental Policy, London SW7 1NA, UK. [2]Imperial College London, Imperial College Business School, Finance Department, London SW7 2AZ, UK. [3]Ecole Normale Supérieure, Paris, Geosciences Department and Environmental Research and Teaching Institute, F-75230 Paris Cedex 05, France. [4]University of California, Los Angeles, Department of Atmospheric and Oceanic Sciences and Institute of Geophysics and Planetary Physics, Los Angeles, California 90095-1565, USA. [5]The World Bank, Agriculture and Environmental Services Department, Risk and Markets Practice, Washington DC 20433, USA. *e-mail: erik.chavez07@imperial.ac.uk

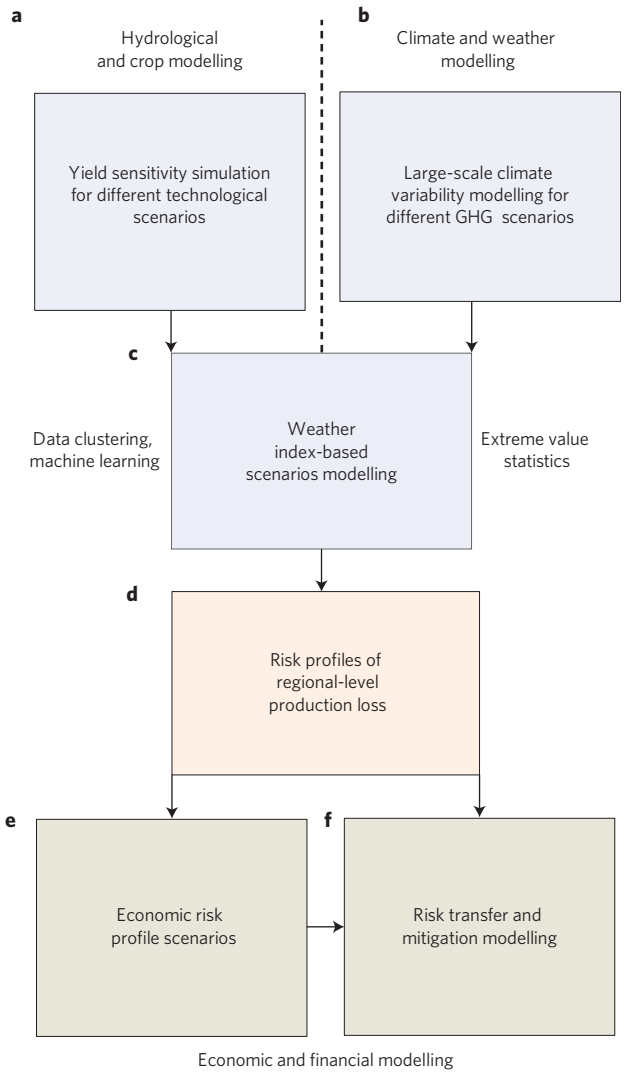

Figure 1 | Schematic diagram of the end-to-end methodology for deriving crop production and economic-risk profiles. a,**b**, Provide hydrological and crop modelling (**a**) and climate and weather modelling (**b**). **c**, Input from **a** and **b** is used to produce grid-to-province PDFs of yield loss captured by weather indices, conditional on large-scale interannual climate processes. **d**, The grid-level yield loss PDFs and yield response functions subject to GHG and technological scenarios from **c** are used to derive regional-level risk profiles of production loss. **e**, If the region matches an economic administrative unit (for example, province, country), the input from **d** is used to to derive distributions of province-level economic losses. **f**, Uses the input from **d** and/or, if relevant, **e**, to determine optimum combinations of risk mitigation and transfer instruments to minimize risk of climate-driven losses.

Supplementary Fig. 2. Finally, complete province-level profiles of economic-loss risk were obtained by considering several technological scenarios for climate risk mitigation. Although a historical climate scenario is presented here, the same methodological construct is applicable to obtain risk profiles in future climate scenarios by using NHMM covariates from simulated large-scale climate drivers.

Vulnerability of crops to weather variability is a sensitive function of growing period. The length of this period and the dates of occurrence of phenological stages, such as flowering and maturity, is also constrained by local weather variability and by environmental conditions, as well as by genetic traits. In addition to extreme weather events, slight changes in planting season and duration of weather patterns may also reduce yields[19]. The weather indices are used to capture the response of crop growth to different features of weather variability. Excess heat indices are built by counting the number of days where the maximum temperature, T_{max}, surpasses a critical threshold, T_c, of 30 or 35 °C—for instance, the number of days with $T_c > 30$ °C from day 10 to day 40 of crop development. Precipitation deficit indices account for cumulative rainfall during a given period of crop growth. The different periods of aggregation of weather indices and the colour code used in Fig. 2 are described in Supplementary Methods and Supplementary Fig. 3.

The machine learning methodology applied here to select pixel-level weather indices shows that the weather indices which best capture weather-driven yield variability exhibit spatial heterogeneity relative to the portion of the growing cycle accounted for by the index. For instance, the optimal indices for the effects of precipitation variability (Fig. 2a) and excess heat (Fig. 2b) on maize yield variability in the northeastern province of Shandong are heterogeneous, with several pixels spatially clustered according to different periods of the growing season (Supplementary Fig. 3) during which the crop is most sensitive to climatic effects. The spatial clustering of indices seems to follow topographical features of Shandong province. For instance, the central mountainous and the westernmost regions of the province are dominated by precipitation indices capturing vulnerability during, respectively, the middle and the end of the crop development. This spatial pattern of precipitation indices also depends on the technological scenario considered (that is, local rain-fed variety, local irrigated variety, switched rain-fed variety), as shown in Supplementary Fig. 4. In contrast, a marked spatial homogeneity is observed in the critical temperature chosen to build heatwave indices. For each pixel, two sets of 25 heatwave indices, with either 30 or 35 °C as critical temperature, were used to determine the optimum heatwave index. It is the 30 °C threshold that is homogeneously chosen across all of Shandong province (figure not shown).

Heatwave-driven variability in rice yield in the Southern provinces of Guangxi and Guangdong possesses similar spatial variability; see Supplementary Figs 5a,b. Estimated impacts of weather variability and climate change on crop production are usually based on IAMs which imply spatially homogeneous hydrometeorological indicators[20]. Doing so is likely to underestimate local-to-regional yield losses. In effect, the rate of succession of phenological growth stages in crops depends on the accumulation of temporal photo-thermal units[21]; this accumulation, in turn, depends on the interaction of local environmental variables. Therefore, the use of homogeneous hydrometeorological indicators may fail to systematically capture times of peak vulnerability, for example, during reproductive stages that vary with location.

Results obtained for northern Shandong (Fig. 2) and Hebei (not shown) provinces illustrate the importance of modelling the joint impacts of precipitation variability and excess temperature stresses on rain-fed crops. Under the baseline scenario of the rain-fed maize variety grown at present, average yield variation throughout Shandong province, subject to the stress of precipitation variability alone, produces slightly positive yield anomalies, whereas the joint modelling of excess temperature and precipitation variability leads to spatially homogeneous negative anomalies. Supplementary Fig. 4 illustrates the latter.

The nonlinearity of maize yield losses due to drought and heat stress is captured by our modelling and is consistent with agricultural field studies[22,23]. The relatively homogeneous yield losses for irrigated rice subject to increasing heatwave exposure throughout the southern Guangdong (not shown) and Guangxi provinces in Supplementary Fig. 5 are consistent with existing literature[24,25], and might actually be underestimated[26].

The results demonstrate that important variations in province-level risk profiles depend on the regional features of weather and climate variability.

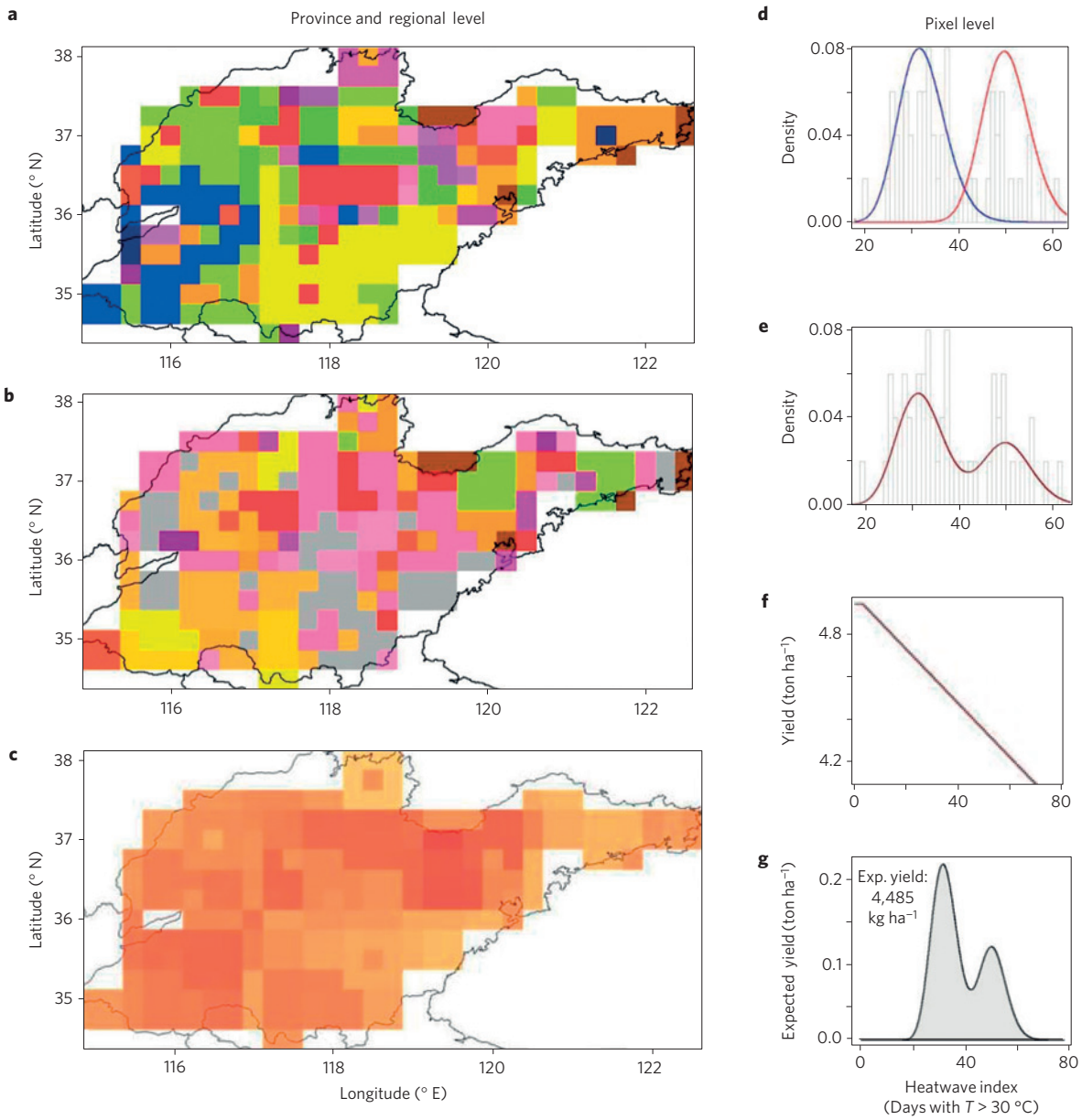

Figure 2 | Results of weather index-based modelling of maize yield in Shandong province. a,**b**, Maps of indices selected to best capture on a 0.25° × 0.25° longitude–latitude grid deficit precipitation (**a**) and excess temperature-driven yield variability (**b**). Colour scale (see Supplementary Fig. 3) indicates the phase of crop growth in which the selected index captures the highest sensitivity. **c**, Map of 10-year return period production (see Methods) of ~200 to ~1,400 tons per pixel (lightest orange to darkest orange in linear colour scale). **d**–**g**, Computations for a heatwave index. **d**, Mixed univariate distributions of the index, subject to each NHMM state. **e**, Viterbi-weighted sum of each distribution. **f**,**g**, Convolution of the response function of yield to heatwave (**f**), with the weighted sum in **e** allows the distribution of yield to be obtained (**g**). Results shown for a single local maize variety rain-fed technological scenario.

To capture dependence on large-scale, low-frequency climate variability, we have constructed and applied an NHMM (ref. 18); see Methods and Supplementary Fig. 6. In the northeastern provinces of Shandong (Fig. 3) and Hebei (not shown), the effect of low-frequency climate change, modelled by this NHMM, is masked by high-frequency weather variability. In fact, northeastern China is strongly affected by mid-latitude weather systems, as well as by teleconnections from the Tropical Pacific[27,28].

In contrast, for the southern Guangdong and Guangxi provinces, risk driven by weather variability depends strongly on the climate state. For a given state, the risk profiles in the southern provinces exhibit minimum variation for varying return periods of weather events, whereas drastic jumps, of 0.18% and 1.15%, in losses of provincial gross domestic product (GDP) occur in Guangdong and Guangxi, respectively, as central-Eastern Pacific sea surface temperatures shift from a warm to a cold event, as captured by the Niño-3.4 index in our NHMM (ref. 29) and illustrated in Supplementary Figs 6 and 7.

We have considered three different technological scenarios: continuing use of a local rain-fed variety, switching to another, more drought tolerant rain-fed variety, and the use of a local irrigated variety. Their effects on the risk profiles are illustrated in Fig. 3a and Supplementary Fig. 4.

The probabilistic risk profiles of economic loss obtained by the present methodology are strongly driven by the physical-loss risk. But the different magnitudes of aggregated direct and indirect losses also reflect the shares of agriculture within each province's GDP (Fig. 3a,b).

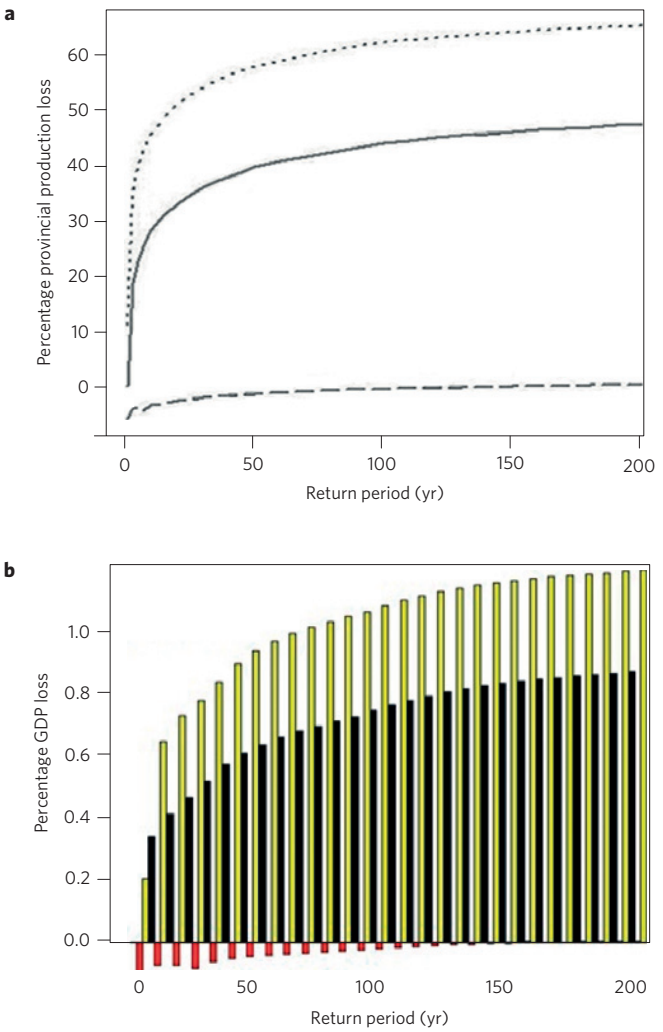

Figure 3 | Risk profiles of province-level physical production and aggregate economic loss in China's northeast Shandong province. a, Risk profiles of maize provincial production loss, driven by the joint impacts of excess temperature and precipitation variability, subject to three different technological scenarios: continuous line, local rain-fed variety; dotted line, switched rain-fed variety; long-dashed line, local irrigated variety. **b**, Risk profiles of direct and indirect aggregate economic loss expressed as a percentage of provincial gross domestic product (GDP_{2008}): black bars, local rain-fed variety; yellow bars, switched rain-fed variety; red bars, local irrigated variety.

Our results should help formulate fiscal policy and public budgeting for these extreme weather risks. Risk management instruments can be used to minimize and cap the cost of weather and climate impacts on society, government and producers.

Investments in infrastructure that increases physical resilience are effective in mitigating risk[30]. Our results indicate a maize production loss generated by a 1-in-50-year event of excess temperature and precipitation variability produces an aggregate 0.7% loss of Shandong provincial GDP (see Fig. 3b). They also indicate that in an irrigation scenario, production and aggregate economic losses are cancelled. As shown in Supplementary Table 1, estimations of the cost of deploying new irrigation infrastructure and restoring existing decaying structures could be performed at a cost of up to 0.73% of Shandong GDP.

The economic efficiency of risk-mitigating investments decreases, however, with the risk level considered and is only justifiable up to certain risk level[31]. To manage the residual risk, instruments of risk transfer and risk forecast can decrease the ex-post event costs of damage.

We propose a 'three-pillar'-based approach for rural development and food security risk management. The three pillars are: risk mitigation, risk forecast and risk transfer instruments. These need to be tailored and combined to respond to specific climate risk profiles characterizing a given region. We believe the results of the end-to-end probabilistic risk assessment methodology presented here will be particularly effective in setting the balance of these three pillars. The implications of this work are of concern for farmers and policy makers, as well as for the whole value chain of the food-and-fibre industry, and for its long-term sustainability. The crucial importance of providing such detailed end-to-end information to stakeholders is further summarized in the Supplementary Discussion.

Methods

Methods and any associated references are available in the online version of the paper.

Received 4 November 2014; accepted 15 June 2015; published online 3 August 2015

References

1. IPCC *Climate Change 2013: The Physical Science Basis* (eds Stocker, T. F. *et al.*) (Cambridge Univ. Press, 2013).
2. Conway, G. *One Billion Hungry: Can We Feed the World?* (Cornell Univ. Press, 2012).
3. Asseng, S. *et al.* Uncertainty in simulating wheat yields under climate change. *Nature Clim. Change* **3,** 827–832 (2013).
4. Challinor, A. J. *et al.* A meta-analysis of crop yield under climate change and adaptation. *Nature Clim. Change* **4,** 287–291 (2014).
5. Moore, F. C. & Lobell, D. B. Adaptation potential of European agriculture in response to climate change. *Nature Clim. Change* **4,** 610–614 (2014).
6. Overpeck, J. T., Meehl, G. A., Bony, S. & Easterling, D. R. Climate data challenges in the 21st century. *Science* **331,** 700–702 (2011).
7. Knutti, R. & Sedláèk, J. Robustness and uncertainties in the new CMIP5 climate model projections. *Nature Clim. Change* **3,** 369–373 (2013).
8. Hannart, A., Ghil, M., Dufresne, J.-L. & Naveau, P. Disconcerting learning on climate sensitivity and the uncertain future of uncertainty. *Climatic Change* **119,** 585–601 (2013).
9. Kunreuther, H. *et al.* Risk management and climate change. *Nature Clim. Change* **3,** 447–450 (2013).
10. Martinson, D. G. *et al.* (eds) *Natural Climate Variability on Decade-to-Century Time Scales* 630 (National Academy Press, 1995).
11. Ghil, M. *et al.* Extreme events: Dynamics, statistics and prediction. *Nonlin. Process. Geophys.* **18,** 295–350 (2011).
12. Ghil, M. & Robertson, A. W. "Waves" vs. "particules" in the atmosphere's phase space: A pathway to long-range forecasting? *Proc. Natl Acad. Sci. USA* **99,** 2493–2500 (2002).
13. Chang, C. P., Ghil, M., Latif, M. & Wallace, J. M. (eds) *Climate Change: Multidecadal and Beyond* (World Scientific/Imperial College Press, in the press).
14. Rosenzweig, M. R. & Binswanger, H. P. *Wealth, Weather and the Composition and Profitability of Agricultural Investment* 42 (The World Bank Policy Research Working Paper, WPS 1055, 1992).
15. Stern, N. *The Stern Review on the Economics on Climate Change* (Cambridge Univ. Press, 2007).
16. Nordhaus, W. D. & Boyer, J. *Warming the World: Economic Models of Global Warming* (MIT Press, 2000).
17. Deloncle, A., Berk, R., D'Andrea, F. & Ghil, M. Weather regime prediction using statistical learning. *J. Atmos. Sci.* **64,** 1619–1635 (2007).
18. Ihler, A. T., Kirshner, S., Ghil, M., Robertson, A. W. & Smyth, P. Graphical models for statistical inference and data assimilation. *Physica D* **230,** 72–87 (2007).
19. Läderach, P. *et al. Mesoamerican Coffee Building a Climate Change Adaptation Strategy* (International Center for Tropical Agriculture Policy Brief No. 2, 2013).
20. Joshi, M. M., Turner, A. G. & Hope, C. The use of land-sea warming contrast under climate change to improve impact metrics. *Climatic Change* **117,** 951–960 (2013).
21. Sanchez, B., Rasmussen, A. & Porter, J. Temperatures and the growth and development of maize and rice: A review. *Glob. Change Biol.* **20,** 408–417 (2014).
22. Lobell, D. B. & Burke, M. B. Why are agricultural impacts of climate so uncertain? The importance of temperature relative to precipitation. *Environ. Res. Lett.* **3,** 034007 (2008).

23. Lobell, D. B., Bänzinger, M., Mogorokosho, C. & Bindiganavile, V. Nonlinear heat effects on African maize as evidenced by historical yield trials. *Nature Clim. Change* **1,** 42–45 (2011).
24. Cheng, W., Sakai, H., Yagi, K. & Hasegawa, T. Combined effects of elevated [CO_2] and high night temperature on carbon assimilation, nitrogen absorption, and the allocations of C and N by rice (Oryza sativa L.). *Agric. Forest Meteorol.* **150,** 1174–1181 (2010).
25. Mohammed, A. R. & Tarpley, L. High night time temperatures affect rice productivity through altered pollen germination and spikelet fertility. *Agric. Forest Meteorol.* **149,** 999–1008 (2010).
26. Sheehy, J. E., Mitchell, P. L. & Ferrer, A. B. Decline in rice grain yields with temperature: Models and correlations can give different estimates. *Field Crop. Res.* **98,** 151–156 (2006).
27. Chang, C.-P. (ed.) *East Asian Monsoon* (World Scientific, 2004).
28. Ding, Y. & Chan, J. C. L. The East Asian summer monsoon: An overview. *Meteorol. Atmos. Phys.* **89,** 117–142 (2005).
29. NOAA *Historical El Niño/La Niña episodes* (*1950–present*); http://www.cpc.ncep.noaa.gov/products/analysis_monitoring/ensostuff/ensoyears.shtml
30. Michel-Kerjan, E. *et al.* Catastrophe risk models for evaluating disaster risk reduction in investments in developing countries. *Risk Anal.* **33,** 984–998 (2013).
31. Mechler, R. & Islam, N. in *The Economic Impacts of Natural Disasters* (eds Guha-Sapir, D., Santos, I. & Borde, A.) 80–106 (Oxford Univ. Press, 2013).

Acknowledgements

T. Jiang and M. Gemmer of the National Climate Centre of the China Meteorological Administration shared the gridded weather data, C. Yang of the Chinese Academy of Mathematics and System Sciences communicated the provincial input–output tables, and simulated crop data was shared by W. Xiong of the Chinese Academy of Agricultural Sciences. It is a pleasure to thank M. Vrac and P. Naveau of the Laboratoire des Sciences du Climat et de l'Environnement, as well as Maarten Speekenbrink of University College London for many helpful discussions. The work of E.C. was supported by the CONACyT, Mexico, and by the Grantham Institute for Climate Change, Imperial College London. M.G. acknowledges support from the US Department of Energy, grant DE-SC0006694, and from the US National Science Foundation, grant OCE-1243175.

Author contributions

E.C., G.C. and M.G. designed the study. E.C. obtained the data and carried out the calculations. M.S. provided further insights into the application of risk profiles to market practice. All four authors contributed to the writing.

Additional information

Supplementary information is available in the online version of the paper. Reprints and permissions information is available online at www.nature.com/reprints. Correspondence and requests for materials should be addressed to E.C.

Competing financial interests

The authors declare no competing financial interests.

Methods

Data sources. Daily observed weather data on precipitation, radiation, and maximum and minimum temperatures were used. The data set was provided by the National Climate Centre (NCC) of the China Meteorological Administration (CMA) on a $0.25^\circ \times 0.25^\circ$ longitude–latitude grid, available from 1961 to 2012; it covered the two northeastern provinces of Shandong and Hebei, and the two southern provinces of Guangxi and Guangdong. Grid-level maize and rice yields were simulated in those northeastern and southern provinces, respectively, using a mechanistic crop model called DSSAR-CERES.

Random-forest-based selection of indices. We selected the most effective pixel-level pairs of indices to capture the effects of deficit precipitation and excess temperature on yield variability by a random-forest algorithm. This algorithm uses ensemble-based recursive partitioning and thus permits one to circumvent the issues of cross-correlation between indices and of a large number of variables versus a small sample size.

Extreme-value multivariate modelling. Robust stochastic characterization of the interannual variability of the optimum grid-level weather indices was carried out using univariate distributions of mixed, exponential—generalized Pareto distribution (GPD)—type. The latter allows one to accurately estimate the risk of occurrence of events that are both rare and extreme, within a modified GPD framework across the whole gridded domain studied. The stochastic dependence of deficit precipitation and excess temperature is characterized by coupling their univariate mixed distributions F_X and F_Y within a Gumbel–Hougaard copula model, as described in the equations (1) and (2) below.

$$F(X,Y) = C_\theta(F_X, F_Y) \tag{1}$$

Here C_θ is the Gumbel–Hougaard Archimedean extreme-value copula,

$$C_\theta = \left\{ -\left(((-\log(u_X))^\theta + (-\log(u_Y))^\theta)^{-1/\theta} \right) \right\} \tag{2}$$

The coefficient of dependence is $\theta \geq 1$, where $\theta = 1$ characterizes independence of the uniform transforms u_X and u_Y of the mixed univariate F_X and F_Y distributions of precipitation and heatwave grid-level indices, respectively.

The Gumbel–Hougaard Archimedean copula enables us to characterize dependence in both the upper and lower tails without assuming independence of extreme-value occurrences, as is the case in Gaussian copulas. An example of stochastic dependence of two weather indices, at the same location and subject to a technological scenario, is presented in Supplementary Fig. 2.

Nonhomogeneous Hidden Markov Model 'weather-within-climate' modelling. Historical univariate or multivariate distributions of weather indices are derived by adopting a 'weather-within-climate' modelling framework. The distributions are modelled conditionally on hidden regional weather states, S_t, that capture seasonal variability. These states are conditioned themselves on observed or simulated continental- and planetary-scale climate drivers that capture interannual modes of variability. A Nonhomogeneous Hidden Markov Model (NHMM) is used to achieve this two-step conditioning and enable the introduction of non-stationarity, as illustrated in Supplementary Fig. 1 across a gridded domain and equation (3) below.

The weather index distributions, $P(O_{1:T}, S_{1:T}|\lambda, z_{1:T})$, thus use continental-scale climate variables, $z_{1:T}$; these covariates can be observed, as done here, or be simulated by high-end general circulation models, subject to future greenhouse gas scenarios.

The non-stationary univariate distributions of pixel-level precipitation and excess heat, $O_{1:T}$, follow the mixed GPD-exponential univariate framework presented above. The copula-characterized stochastic dependency between marginals is considered stationary across weather states.

Here $1961 \leq t \leq 2012$, S_t are the hidden states of the two-state Markov chain, z_t is the non-stationary Niño-3.4 index acting as covariate, $\lambda = \{a_i, \pi_i\}_{i=\{1,2\}}$ contains the transition parameters a_i and initial probabilities π_i of the NHMM, and b_{S_t} is the distribution of the observed weather indices at time t, depending on the state S_t as follows:

$$P(O_{1:T}, S_{1:T}|\lambda, z_{1:T}) = \pi_i(z_1) b_{S_1}(O_1|z_1) \prod_{t=1}^{T-1} a_{ij}(z_t) b_{S_t}(O_{t+1}|z_{t+1}) \tag{3}$$

where $a_{ij}(z_t)$ is the transition probability from state i at time t to j at time $t+1$ of a first-order Markov chain as a function of the non-stationary covariate z_t, $\pi_i(z_1)$ is the probability that the initial hidden state at $t = 1$ is i, $S_1 = i$, and $b_{S_t}(O_{t+1}|z_{t+1})$ is a component of the vector of observed weather indices characterized by mixed densities F_X and F_Y cited above, and dependent on the value of the non-stationary covariate z_{t+1}.

Generalized additive mixed crop response modelling. To model the vulnerability functions of crop yield to the combined or individual effects of precipitation variability and excess temperature exposure, generalized additive mixed models (GAMMs) are used (see equation (4)). The use of a GAMM $g(\mu_i)$ enables one to capture the nonlinear response of crop yield μ_i to varying values of a single or several weather indices (see Fig. 2f),

$$g(\mu_i) = X_i\theta + f_1(x_{1i}) + f_2(x_{2i}) + \cdots \tag{4}$$

Here $\mu_i \equiv E(Y_i)$, with Y_i the rice or maize yield response variable following an exponential-family probability distribution function, and X_i is the ith row of the model matrix with its corresponding θ parameter vector.

Also, to model the univariate model of rice or maize yield response to heatwaves or deficit precipitation, a smoothing basis composed of natural cubic splines is used. Ultimately, the convolution of the GAMM-based yield response function with the distribution of the corresponding grid-level indices results in the distribution of yield loss as a function of index values.

Input–output-based economic impact modelling. An input–output modelling approach is used to assess direct and indirect province-level economic impacts due to weather-driven maize production shortfall. Further details concerning the methodology can be found in the Supplementary Information.